San Jose State University

SJSU ScholarWorks

1-1-2013

An inventory of the stellar initial mass function in early-type galaxies

C. Tortora
Institut für Theoretische Physik

Aaron J. Romanowsky
San Jose State University, aaron.romanowsky@sjsu.edu

N. R. Napolitano
INAF-Osservatorio Astronomico di Capodimonte

Follow this and additional works at: https://scholarworks.sjsu.edu/physics_astron_pub

Part of the Astrophysics and Astronomy Commons

Recommended Citation

AN INVENTORY OF THE STELLAR INITIAL MASS FUNCTION IN EARLY-TYPE GALAXIES

C. TORTORA[1], A. J. ROMANOWSKY[2,3], AND N. R. NAPOLITANO[4]

[1] Institut für Theoretische Physik, Universität Zürich, Winterthurerstrasse 190, CH-8057 Zürich, Switzerland; ctortora@physik.uzh.ch
[2] University of California Observatories, 1156 High Street, Santa Cruz, CA 95064, USA
[3] Department of Physics and Astronomy, San José State University, One Washington Square, San Jose, CA 95192, USA
[4] INAF-Osservatorio Astronomico di Capodimonte, Salita Moiariello 16, I-80131 Napoli, Italy

ABSTRACT

Given a flurry of recent claims for systematic variations in the stellar initial mass function (IMF), we carry out the first inventory of the observational evidence using different approaches. This includes literature results, as well as our own new findings from combined stellar population synthesis (SPS) and Jeans dynamical analyses of data on ∼4500 early-type galaxies (ETGs) from the SPIDER project. We focus on the mass-to-light ratio mismatch relative to the Milky Way IMF, $\delta_{\rm IMF}$, correlated against the central stellar velocity dispersion, $\sigma_\star$. We find a strong correlation between $\delta_{\rm IMF}$ and $\sigma_\star$, for a wide set of dark matter (DM) model profiles. These results are robust if a uniform halo response to baryons is adopted across the sample. The overall normalization of $\delta_{\rm IMF}$ and the detailed DM profile are less certain, but the data are consistent with standard cold DM halos and a central DM fraction that is roughly constant with $\sigma_\star$. For a variety of related studies in the literature, using SPS, dynamics, and gravitational lensing, similar results are found. Studies based solely on spectroscopic line diagnostics agree on a Salpeter-like IMF at high $\sigma_\star$ but differ at low $\sigma_\star$. Overall, we find that multiple independent lines of evidence appear to be converging on a systematic variation in the IMF, such that high-$\sigma_\star$ ETGs have an excess of low-mass stars relative to spirals and low-$\sigma_\star$ ETGs. Robust verification of super-Salpeter IMFs in the highest-$\sigma_\star$ galaxies will require additional scrutiny of scatter and systematic uncertainties. The implications for the distribution of DM are still inconclusive.

Key words: galaxies: elliptical and lenticular, cD – galaxies: evolution – galaxies: general

Online-only material: color figures

1. INTRODUCTION

The stellar initial mass function (IMF) is fundamentally important to understanding both stellar populations and galaxies. The Milky Way (MW) IMF was originally characterized as a power-law mass distribution, $dN/dM \propto M^{-\alpha}$, with $\alpha \sim 2.35$ (Salpeter 1955), and subsequently refined to flatten at lower masses ($M \lesssim 0.5\,M_\odot$; Kroupa 2001; Chabrier 2003).

Whether or not the MW IMF describes stellar populations elsewhere in the universe cannot yet be said through direct star counts. There have been some indirect observational hints of IMF variations and ample theoretical motivation for these, but no broadly convincing evidence has emerged (cf. Bastian et al. 2010).

This situation has recently changed, with a flurry of studies of early-type galaxies (ETGs) turning up indirect evidence for systematic IMF variations. These studies use models of stellar population synthesis (SPS) to fit integrated-light data (broadband colors and spectroscopic features) and fall into two broad categories: "pure" SPS and "hybrid" SPS+gravitating mass analyses.

The pure analyses rely on spectral lines that are differentially sensitive to giant or dwarf stars. These include the TiO feature at 6130 Å, the Na I doublet near 8190 Å, the Ca II triplet near 8600 Å, the Wing–Ford [Fe/H] band at 9915 Å, and the Ca I line at 10345 Å (e.g., Cenarro et al. 2003; van Dokkum & Conroy 2010; Spiniello et al. 2012; Conroy & van Dokkum 2012, hereafter CvD12; Ferreras et al. 2013; Smith et al. 2012).

The hybrid analyses assume an IMF and infer a stellar mass-to-light ratio $\Upsilon_\star$ using a more conventional SPS approach based on colors and age- and metallicity-sensitive spectral lines. Estimates of $\Upsilon_\star$ are also derived using dynamics or gravitational

lensing. Comparison of the independent results then yields a revised IMF (e.g., Cappellari et al. 2006, 2012a, 2012b; Ferreras et al. 2008; Tortora et al. 2009, 2010, 2012; Grillo & Gobat 2010; Grillo 2010; Treu et al. 2010; Napolitano et al. 2010, 2011; Auger et al. 2010; Thomas et al. 2011; Spiniello et al. 2011; Dutton et al. 2012a, 2012b; Sonnenfeld et al. 2012; Wegner et al. 2012).

One may characterize a revised IMF through its $\Upsilon_\star$ relative to an MW disk IMF, $\delta_{\rm IMF} \equiv \Upsilon_\star/\Upsilon_{\star,\rm MW}$ (the "mismatch parameter"), where for reference we adopt the Chabrier IMF. Remarkably, almost all the above studies found "heavy" IMFs ($\delta_{\rm IMF} \gg 1$) for the most massive ETGs. Less massive ETGs and spiral galaxies appear to have "normal/light" IMFs ($\delta_{\rm IMF} \lesssim 1$; e.g., Bell & de Jong 2001; Bershady et al. 2011; Suyu et al. 2012; Brewer et al. 2012), and the bulge components of spirals may also have a similar mass dependence to ETGs (de Blok et al. 2008; Ferreras et al. 2010, hereafter F+10; Dutton et al. 2013, hereafter D+13).

These IMF findings are both potentially revolutionary and highly controversial and demand further investigation. In particular, with hybrid analyses there are lingering questions about degeneracies associated with the distribution of non-baryonic dark matter (DM). The time is also ripe to inventory the results to date and see if the apparent emerging consensus holds up under quantitative, systematic comparison—which could provide pressing motivation for understanding the physical origins of the trends. Comparisons were made for some hybrid analyses (Thomas et al. 2011; Dutton et al. 2012a; Wegner et al. 2012), but not for the pure SPS work.

In this paper we carry out such an inventory, while presenting our own novel results for a large sample of ETGs for reference, following the dynamical+SPS analyses of Tortora et al. (2012,

hereafter T+12). We focus on the trends in δ_{IMF} with central stellar velocity dispersion, $\sigma_\star$, and discuss some implications for the central DM fraction. $\sigma_\star$ is widely considered as crucially connected to galaxy evolution and, unlike $\Upsilon_\star$, is relatively independent of the bandpass and of δ_{IMF}.

We describe our data and analysis methods in Section 2. We present our results in Section 3 and make literature comparisons in Section 4. We summarize the conclusions and outlook in Section 5.

2. DATA AND ANALYSIS METHODS

We apply a combination of SPS and stellar dynamical models to a sample of $\sim$4500 giant ETGs, in the redshift range of $z = 0.05$–0.1, drawn from the SPIDER project (La Barbera et al. 2010b). Our data include optical+near-infrared photometry [from the Sloan Digital Sky Survey (SDSS) and the UKIRT Infrared Deep Sky Survey-Large Area Survey],[5] high-quality measurements of galactic structural parameters (effective radius R_e and Sérsic index n), and SDSS central-aperture velocity dispersions σ_{Ap}. The sample galaxies are defined as bulge-dominated systems with passive spectra, while late-type systems are efficiently removed through the SDSS classification parameters based on the spectral type and the fraction of light that is better described by a de Vaucouleurs (1948) profile (see T+12 for further details). The structural parameters are measured using 2DPHOT (La Barbera et al. 2008) and are found to be significantly different from the SDSS estimates (La Barbera et al. 2010b). The sample is 95% complete at a stellar mass of $M_\star = 3 \times 10^{10}\ M_\odot$, which corresponds to $\sigma_{Ap} \sim 160\ \mathrm{km\,s^{-1}}$.

The SPS-based $\Upsilon_\star$ values were derived by fitting Bruzual & Charlot (2003) models to the multi-band photometry, assuming a Chabrier IMF. These results have been shown to be consistent with independent literature (e.g., MPA masses in Dutton et al. 2012a), while possible systematics in stellar mass ($M_\star$) estimates are discussed in Swindle et al. (2011) and T+12. Despite the well-known age–metallicity degeneracies in photometric data, these conspire to keep the stellar mass-to-light ratio well constrained, with scatter of 0.05–0.15 dex. The agreement is also excellent when our color-derived masses are compared with spectroscopic estimates. The largest systematical uncertainty in our analysis comes from our ignorance about the IMF shape, which can produce variations of the stellar M/L of a factor as large as $\sim$2. For this reason the IMF is a key issue in stellar population analysis and the central topic of this paper.

Our dynamical-mass estimates use spherical isotropic Jeans equations fitted to the σ_{Ap} data. We also extend the T+12 analysis using two-component mass models: a Sérsic-based stellar distribution following the K-band light, and a standard DM profile. For the latter we adopt a series of plausible assumptions (cf. Cappellari et al. 2012a), as the data do not allow us to constrain both components simultaneously.

Our DM models are based on the Navarro et al. (1996, hereafter NFW) profile, with an adjustable degree of baryon-induced adiabatic contraction (AC). For the virial mass and concentration (M_{vir}, c_{vir}), we adopt mean trends for a WMAP5 cosmology (Macciò et al. 2008), and for the M_{vir}–$M_\star$ relation we used Moster et al. (2010, hereafter M+10). Each galaxy's mass model then has one free parameter, $\Upsilon_\star$, plus optional AC (Gnedin et al. 2004, hereafter G+04), providing our no-AC-NFW and AC-NFW base models.

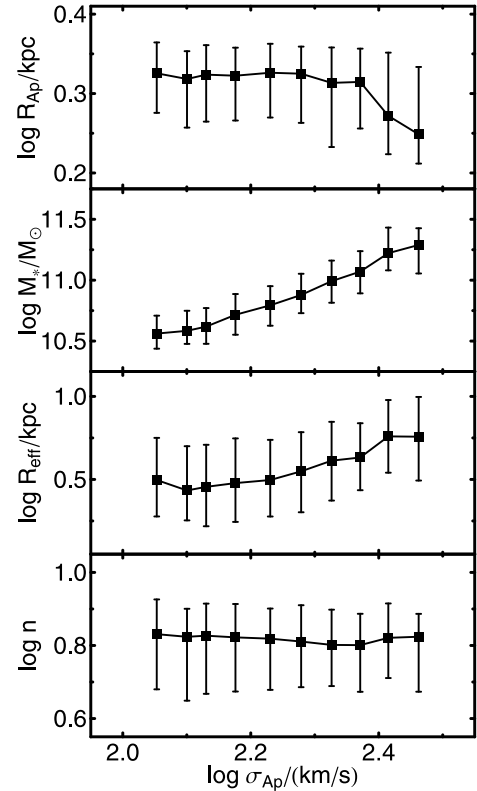5 http://www.sdss.org, http://www.ukidss.org

Figure 1. Galaxy sample properties, binned by velocity dispersion: physical aperture radius, SPS-based stellar mass (Chabrier IMF), effective radius, and Sérsic index. The points and error bars show the medians and 25–75 percentile scatter.

We explore the sensitivity of our results to these assumptions by doing the analyses with the following alternatives: (1) AC recipes of varying strengths (Blumenthal et al. 1986, hereafter B+86; Abadi et al. 2010, hereafter A+10); (2) M_{vir} with a fixed value for the entire sample: $M_{vir} = 10^{12}\ M_\odot$, $10^{13}\ M_\odot$, or $10^{14}\ M_\odot$; (3) WMAP3-based c_{vir}–M_{vir} relation (Macciò et al. 2008); (4) no DM is present; (5) mild kinematic anisotropy, with $\beta = -0.2$ or $+0.2$; (6) c_{vir}–M_{vir} relation altered to mimic a warm dark matter (WDM) cosmology, assuming different particle masses (Schneider et al. 2012, hereafter S+12a).

To study the mean trends of $\Upsilon_\star$ with velocity dispersion, we construct "average" galaxies by dividing our sample into 10 σ_{Ap} bins, for which we compute median values of $M_\star$, R_e, n, R_{Ap}, and σ_{Ap}. We show these values and their 25–75 percentile scatter in Figure 1. For each σ_{Ap}-bin and a given DM model, we solve the radial Jeans equation for the $\Upsilon_\star$ value that matches the observed σ_{Ap}.

Our final analysis products, for each galaxy bin and mass model, will be the SPS-determined $\Upsilon_{\star,MW}$, the dynamically determined $\Upsilon_\star$, the inferred δ_{IMF}, and the inferred central DM fraction, $f_{DM} \equiv 1 - \Upsilon_\star/\Upsilon_{dyn}$. For homogeneity, we convert σ_{Ap} to σ_e (the value at R_e), using the best-fitting relation in Cappellari et al. (2006; also done for the literature results later).

3. RESULTS: IMF AND DM FRACTION TRENDS

Our main IMF results are shown in Figure 2. The two thick black curves correspond to our standard no-AC-NFW (solid) and AC-NFW (long-dashed) models, and the suite of alternative models are also plotted, as labeled.
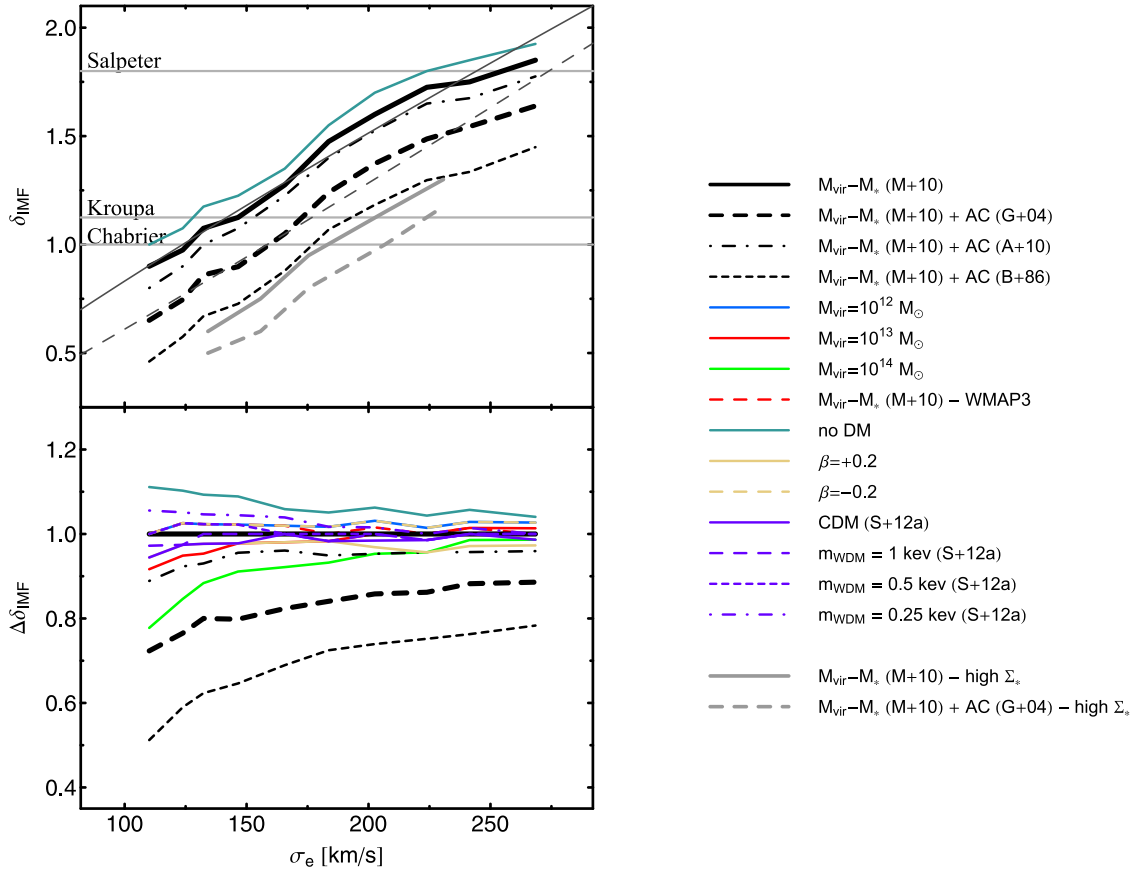
Figure 2. IMF mismatch parameter, $\delta_{\rm IMF} = \Upsilon_\star/\Upsilon_{\star,\rm MW}$, vs. velocity dispersion, σ_e, for the SPIDER sample. Top: results for several different mass models. Horizontal lines show reference values for Salpeter, Kroupa, and Chabrier IMFs (top to bottom). The best-fitted relations for the no-AC-NFW and AC-NFW base models are also shown as thin dark gray lines. Bottom: residuals relative to the fiducial no-AC-NFW result, for an expanded series of mass models (see legend at right, explanation in the main text, and reference list for abbreviations). The overall normalization of $\delta_{\rm IMF}$ depends on the model assumptions, but a steep relation between $\delta_{\rm IMF}$ and σ_e emerges as a robust result.

(A color version of this figure is available in the online journal.)

It is clear that the overall normalization of $\delta_{\rm IMF}$ is degenerate with the adopted halo model, as DM can be traded against stellar mass. This degeneracy is most severe when allowing for uncertainties in the halo response to baryons (more so than with the virial mass assumptions). However, for a given flavor of the halo model, there is always a strong correlation between $\delta_{\rm IMF}$ and σ_e (the $\delta_{\rm IMF}$–$M_\star$ trend is weaker). We quantify this correlation for each model with a log–log fit, reporting the best-fit parameters in Table 1 (also plotted in Figure 2 for the two reference models[6]); the typical relation is $\delta_{\rm IMF} \propto \sigma_e$.

Other models of potential interest are low-density DM cores (Burkert 1995) and alternatives to DM (e.g., Milgrom 1983). These would imply similar $\delta_{\rm IMF}$–σ_e slopes to our limiting no-DM model. The no-DM assumption produces the uppermost curve in Figure 2 and is qualitatively consistent with a slightly *expanded* NFW model. The same results, using the same data set but somewhat different mass modeling assumptions, have been anticipated in Tortora et al. (2012).

One could alter these slopes with additional model tuning; e.g., with strong AC at high σ_e and halo expansion at low σ_e, one could completely flatten out the trend. On the other hand, decreasing the AC at high σ_e and increasing the strength of the AC toward lower σ_e would make the trend even steeper. We currently have no a priori motivation for either direction

Table 1
Best-fit Parameters for the Relation $\log \delta_{\rm IMF} = a + b \log \frac{\sigma_e}{200\,{\rm km\,s}^{-1}}$, for Model Suite (See the Main Text)

Model	a	b
$M_{\rm vir}$–$M_\star$ (M+10)	0.18	0.86
$M_{\rm vir}$–$M_\star$ (M+10) + AC (G+04)	0.11	1.07
$M_{\rm vir}$–$M_\star$ (M+10) + AC (A+10)	0.16	0.93
$M_{\rm vir}$–$M_\star$ (M+10) + AC (B+86)	0.04	1.29
$M_{\rm vir} = 10^{12}\,M_\odot$	0.19	0.88
$M_{\rm vir} = 10^{13}\,M_\odot$	0.18	0.97
$M_{\rm vir} = 10^{14}\,M_\odot$	0.16	1.09
$M_{\rm vir}$–$M_\star$ (M+10), WMAP3	0.18	0.85
No DM	0.21	0.79
$\beta = +0.2$	0.17	0.87
$\beta = -0.2$	0.19	0.88
CDM (S+12a)	0.17	0.90
$m_{\rm WDM} = 1\,{\rm keV}$ (S+12a)	0.18	0.88
$m_{\rm WDM} = 0.5\,{\rm keV}$ (S+12a)	0.18	0.84
$m_{\rm WDM} = 0.25\,{\rm keV}$ (S+12a)	0.19	0.80

for the AC variations, and thus we cannot argue in favor of an IMF universality for the former case or for a very strong IMF non-universality in the latter one.

We next examine the overall IMF normalization, with the no-AC-NFW and AC-NFW cases bracketing the most plausible range of models. For reference, we show $\delta_{\rm IMF}$ predictions for

---

[6] We note that a log–log fit, although crude, is a good approximation of the trends in Figure 2.
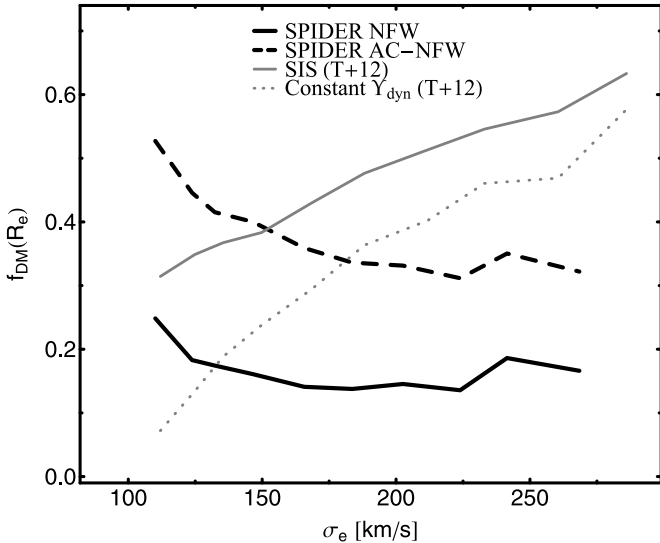
Figure 3. Inferred DM fraction within 1 R_e vs. σ_e, for the SPIDER sample with different modeling assumptions. The solid and dashed black curves are our default no-AC-NFW and AC-NFW models, respectively. The gray curves are for fixed Chabrier IMF, with isothermal and constant-Υ_{dyn} models, bracketing the range of non-parametric models (solid and dotted curves, respectively; see T+12). With standard ΛCDM halos and a variable IMF, f_{DM} is constant or mildly decreasing with σ_e; with a fixed IMF, f_{DM} is strongly increasing (cf. Thomas et al. 2011, Figure 16).

several standard IMFs (Salpeter, Kroupa, Chabrier). We note that at a fixed IMF, age, and metallicity, the $\Upsilon_\star$ and δ_{IMF} values are uniquely predicted, but the reverse is not true. A given δ_{IMF} result can imply multiple IMF solutions, particularly if one allows for mass functions more complicated than a pure power law.

If we adopt a no-AC-NFW model, an MW-like IMF is implied for low-σ_e galaxies and a Salpeter IMF for high-σ_e ones. For AC-NFW, the low-σ_e galaxies have sub-MW IMFs, and the high-σ_e ones have IMFs intermediate to Kroupa and Salpeter.

In all cases, extremely bottom-heavy IMFs (assumed single power law, $\alpha \gtrsim 2.6$) are ruled out, on average. Even if one assumed *no* DM, such IMFs would violate the dynamical constraints on the overall mass-to-light ratio.

Although resolving the remaining IMF–DM degeneracy will require more extensive analysis, we carry out a simple exercise to provide initial clues, inspired by Dutton et al. (2012b). As in that paper, we select the galaxies with mean central stellar surface densities $\Sigma_\star > 2500\,M_\odot\,{\rm pc}^{-2}$ and analyze them the same as the full sample. The rationale is that such galaxies are the most star dominated and the least sensitive to DM uncertainties. The results are shown by the gray curves in Figure 2, where, as expected, the model curves are closer together. The implied δ_{IMF} normalization is fairly low—similar to the full-sample AC results. We may then apply this IMF result to the full sample if we assume no additional systematic δ_{IMF}–$\Sigma_\star$ correlation (cf. Schulz et al. 2010).

Although this paper is primarily concerned with the IMF, we briefly examine some implications for the central DM content. Our main mass models are, by construction, fully consistent with current expectations for ΛCDM halo profiles, while also agreeing with the observations for a plausible IMF range ($\delta_{IMF} \sim$ 0.5–2.0).

We show the implied f_{DM} within 1 R_e in Figure 3. We find fairly universal values of $f_{DM} \sim 0.2$ and ~0.5 for the no-AC-NFW and AC-NFW models, respectively. These results are not altered appreciably in the alternative models explored above.

Note also that the high-$\Sigma_\star$ test above prefers the AC-NFW model.

The figure also shows that if we adopted a constant IMF, then we would infer a strong increase of f_{DM} with σ_e. Such behavior has been invoked as the driver for the "tilt" of the ETG fundamental plane (see Tortora et al. 2009, and references therein), but now with renewed comparison to realistic DM halo models, we find that the tilt is driven at least in part (and perhaps wholly) by the IMF. Put differently, the observed Υ_{dyn}–σ_e relation is too steep to explain through standard DM models and requires an additional factor.

4. LITERATURE COMPARISONS

We now compare our SPIDER-based results with an inventory of other literature results for ETGs in Figure 4 and late-type galaxies in Figure 5.

4.1. Early-type Galaxies

We discuss the results for ETGs in Figure 4, starting with those studies that used similar hybrid approaches, comparing SPS-mass estimates to total mass using dynamics or lensing. Rather than exhaustively comparing all such results, we will focus on the studies that explicitly derived δ_{IMF} for large samples of low-z ETGs.

The study most closely related to ours is Dutton et al. (2012a), who analyzed SDSS data for ETGs (colors and $\sigma_\star$, with SPS+Jeans modeling). Their sample was much larger but without the Sérsic models and near-infrared photometry from SPIDER. Their results for a no-AC-NFW model are shown as a dotted orange curve in panel (a), which is reassuringly similar to our no-AC-NFW result, with the ~30% residual difference in δ_{IMF} illustrating the level of systematic uncertainties for a fixed data set and method. Although a conclusive answer on the origin of this discrepancy is not available, we have found that shallower light profiles (as may be equivalent to the combination of the $n = 1$ and $n = 4$ profiles in Dutton et al. 2012a) produce larger $\Upsilon_\star$. Finally, the solid line shows their refined result from a multi-parameter fit: they found DM halos that are slightly expanded and consequently a slightly heavier IMF.

In panel (b), we show results from the ATLAS[3D] survey of nearby ETGs, using both spectroscopically based SPS models and detailed two-dimensional Jeans dynamical analyses (Cappellari et al. 2012b, where we show their no-AC-NFW results). As with SPIDER, the ATLAS[3D] project found that the overall δ_{IMF} normalization was degenerate to the DM assumptions, but the trend with σ_e was robust. Direct comparison in Figure 4 reveals that these results are consistent with SPIDER within the errors, which is also the case for an earlier study of ETGs with SAURON (Cappellari et al. 2006) and for an analysis of high-z galaxies (Cappellari et al. 2009).

Panel (c) shows results from Thomas et al. (2011) and Wegner et al. (2012), who carried out spectroscopic SPS and detailed orbit modeling of ETGs found in clusters (including Coma), using a variety of mass models (constant-Υ_{dyn}, no-AC-NFW, and cored halos). We see no systematic difference between the results obtained with different mass models. A systematic offset in δ_{IMF} between the two studies is found, but overall the results are consistent with our no-AC-NFW results, both in amplitude and in slope.

Panel (d) shows gravitational lensing results, primarily from the SLACS survey of ETGs (Treu et al. 2010), using no-AC-NFW models, as well as color-based SPS models and
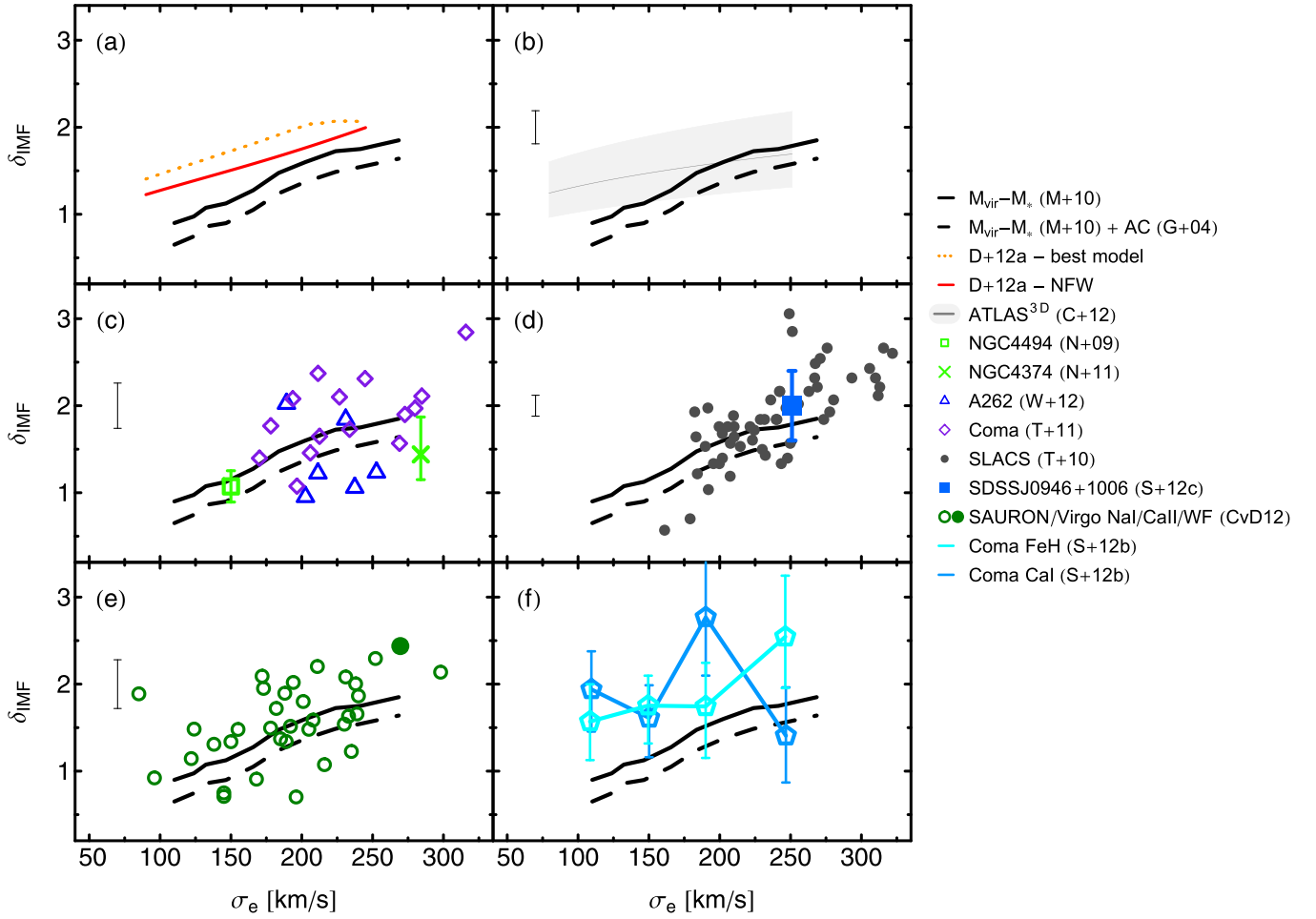
Figure 4. IMF mismatch-parameter vs. stellar velocity dispersion, comparing the SPIDER results (black curves) to various literature studies. These include hybrid results from Dutton et al. (2012a, D+12a), Cappellari et al. (2012b, C+12), Wegner et al. (2012, W+12), Thomas et al. (2011, T+11), and Treu et al. (2010, T+10); SPS ones from Conroy & van Dokkum (2012, CvD12) and Smith et al. (2012, S+12b); and single-galaxy results from Napolitano et al. (2009, N+09), Napolitano et al. (2011, N+11) and Sonnenfeld et al. (2012, S+12c). In several panels, typical error bars are shown to the left. The filled CvD12 datapoint is from four galaxies' stacked spectra. There is generally good consistency in the inferred IMF trends from the different studies.

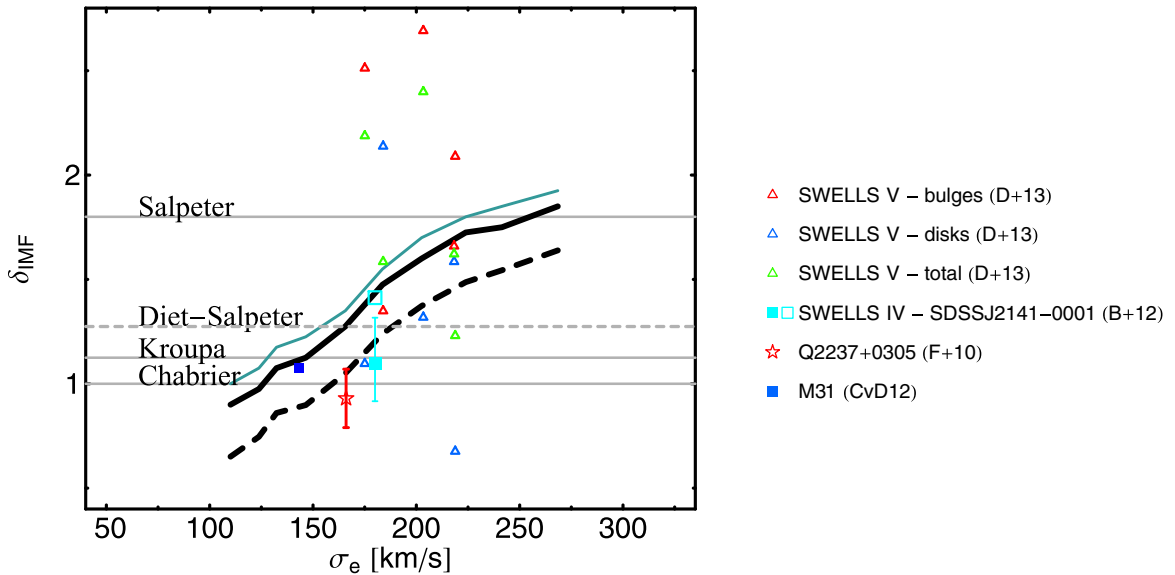(A color version of this figure is available in the online journal.)

Figure 5. IMF mismatch-parameter vs. $\sigma_\star$, comparing the SPIDER results to various literature studies on spiral galaxies. See legend at right for the symbols (and legend in Figure 2 for the curves). Horizontal solid lines show reference values for Salpeter, Kroupa, and Chabrier IMFs, while the dashed one is for the diet Salpeter from Bell & de Jong (2001).

(A color version of this figure is available in the online journal.)

stellar-dynamics constraints. Their δ_{IMF} normalization agrees well overall with ours, but their slope is somewhat steeper.[7]

Our results, along with the four hybrid studies from the literature, all suggest that the IMF of ETGs varies from MW-like at low σ_e to Salpeter-like at high σ_e, modulo some lingering uncertainties from the DM–IMF degeneracy.

In addition to the large-sample studies, we examine a few key single-galaxy results. These include extended kinematics data with NFW-based modeling (Napolitano et al. 2009, 2011), as shown in panel (c), and the "Jackpot" double lens (Sonnenfeld et al. 2012), in panel (d), and all look consistent with the trend from SPIDER.

Our culminating comparisons are with a completely different set of results, based purely on modeling of IMF-sensitive spectral lines (see Section 1). Most of these lines are susceptible to degeneracies with elemental abundances (e.g., sodium or calcium), and we consider only those studies that have directly accounted for such effects.

We first show in panel (e) the results from CvD12. They fitted spectral features across a wide wavelength range, focusing on the IMF indicators Na I, Ca II, and the Wing–Ford band, while adopting a broken-power-law IMF form and fitting for the relevant elemental abundances. Their inferred δ_{IMF} values turn out to agree well with both the normalization and the trend versus σ_e from the SPIDER results (for the no-AC-NFW models in particular).[8] Recalling that the high δ_{IMF} values from hybrid studies could be due to either a bottom-heavy (extra dwarfs) *or* a top-heavy (extra remnants) IMF, the CvD12 results agree with only the first solution.

Note that the apertures probed here are different: $R_e/8$ for CvD12, and 0.3–0.7 R_e for SPIDER (decreasing with $\sigma_\star$). The close agreement of the results on average thus implies that the IMF does not vary spatially on these scales, or that the AC model is the correct solution, and δ_{IMF} decreases with galactocentric radius, which is plausible (e.g., Carter et al. 1986; see also Figure 13 of CvD12).

Panel (f) shows results from Smith et al. (2012), who studied a large sample of Coma-cluster ETGs. They used the same SPS models as CvD12 to fit near-infrared spectroscopic line indices, analyzing the Wing–Ford band and the Ca I line separately. The former line was susceptible to uncertainties in the Na abundance, but not the latter. We have converted their results to inferred δ_{IMF} by straightforward interpolation between the Chabrier, Salpeter, and $\alpha = 3$ models in their Figure 10. The final results are somewhat noisy and uncertain but imply an overall Salpeter-like normalization and no obvious trend with σ_e. This agrees with all the aforementioned results at high σ_e, but not at low σ_e. It is possible that these Coma-cluster galaxies are genuinely different. As environmental classification is part of the SPIDER data set (La Barbera et al. 2010a; La Barbera et al. 2010c; Tortora et al. 2012), we have investigated the impact of environment on our results and found very little effect on δ_{IMF}. But we also have very few cluster galaxies in our sample, and a definitive comparison with those Coma-cluster results is not possible.

Spiniello et al. (2012) analyzed NaD, Na I, and TiO$_2$ lines in SDSS spectra of ETGs with $\sigma_\star > 200$ km s^{-1}, comparing to the same SPS models as CvD12. They inferred a Salpeter-like IMF at low $\sigma_\star$, which is consistent with SPIDER. At high $\sigma_\star$, they inferred $\alpha \sim 3$, which would imply $\delta_{IMF} \sim 4$ and violate the total mass constraints both from SPIDER and from the lens galaxy that these authors also studied. This conflict suggests that either further work is needed on the line-index modeling or the IMF shape deviates from a simple power law.

An ideal comparison with our SPIDER results would be the work of Ferreras et al. (2013), who analyzed Na I and TiO line strengths from the SPIDER parent data set. Although they did not provide δ_{IMF} values that we could compare to our results, their illustrative $\Upsilon_\star$ trends versus $\sigma_\star$ (at fixed metallicity and age) are qualitatively similar. They also demonstrated that the δ_{IMF} inferences in their approach could depend strongly on the detailed shape assumed for the IMF.

4.2. Late-type Galaxies

It would also be fascinating to see whether or not bulges/disks follow the same δ_{IMF}–$\sigma_\star$ trends as ETGs. Unfortunately, although direct inferences from star counts are possible in the Milky Way and nearby galaxies, the literature in the field is not sufficient to investigate with accuracy IMF variations with mass or $\sigma_\star$, if any. However, it appears that a general consensus is arising within the community, which points to Kroupa/Chabrier type. In general, the IMF looks similar in the field, dense massive clusters and diffuse low-density star-forming regions, with some deviations observed in a handful of other regions (see Bastian et al. 2010 and Kroupa et al. 2011 for a review of the main results). Analyses of masses above ~ 1 $M_\odot$ have been performed in nearby galaxies (for instance, the irregular LMC, the dwarf SMC, and the spiral M33), ruling out strong IMF variations. Similarly, starburst galaxies and their embedded young massive clusters imply no IMF variation and no influence of the local environment.

Such analyses provide only limited information on a restricted sample of galaxies. However, in recent years, similarly to the ETGs' case, studies of variations with galaxy mass have been accumulating. For example, Falcón-Barroso et al. (2003) found that bulges of spirals showed anti-correlations between $\sigma_\star$ and Ca II line strengths, similar to ETGs, but they could not determine if this was an IMF effect.

We have attempted to investigate further, using δ_{IMF} inferences for bulges and disks from the literature (e.g., de Blok et al. 2008; F+10; Barnabè et al. 2012, hereafter B+12; CvD12; D+13). This comparison is shown in Figure 5.

Using bulges from de Blok et al. (2008), we find that δ_{IMF} correlates with stellar mass, giving hints of an ETG-like δ_{IMF}–$\sigma_\star$ correlation, but we also find the same for the disks, which would be peculiar. Note that initial results on dynamical masses of nearby spiral disks suggest $\delta_{IMF} \sim 1$ (Bershady et al. 2011; Westfall et al. 2011).

We show the results for a sample of five massive spiral galaxies from Dutton et al. (2013), who found (1) stellar mass carrying out a photometric SPS and (2) an independent IMF estimate, using strong gravitational lensing and gas kinematics. The apparent scatter for both bulges and disks is enormous, suggesting that more work is needed to address the systematic errors and to understand any additional trends with detailed morphology. However, the IMF normalization is higher in the bulges than in the disks.

---

[7] Not all of the analyses of the SLACS data performed by non-SLACS teams agree about the IMF conclusions. But we note that our own analysis in Tortora et al. (2010) agrees with the SLACS-team analysis. Note also that the SPIDER and SLACS samples are selected on luminosity and velocity dispersion, respectively.

[8] CvD12 compared their $\Upsilon_\star$ results to *total* dynamical values from SAURON in order to check that they did not violate those constraints. However, they did not compare to *decomposed* dynamical $\Upsilon_\star$ inferences for consistency as we do here.

A similar analysis has been performed in B+12 (updating the results in Dutton et al. 2011), where gravitational lensing, gas rotation curve, and stellar kinematics for the lens galaxy SDSS J2141−0001 were used. They found a δ_{IMF} that is fully consistent with an intermediate-normalization IMF (in between a Salpeter and a Chabrier IMF), but taking into account the expected cold gas fraction (which had not been included in the fitting procedure), they found lower δ_{IMF}, agreeing with a Chabrier/Kroupa IMF. A bottom-light IMF was also found by F+10, who analyzed the strong-lensing features of the Einstein Cross (Q2237+0305), and Conroy & van Dokkum (2012) using spectral lines in the nuclear bulge of M31.

5. DISCUSSION AND CONCLUSIONS

We have analyzed the dynamics and stellar populations of a large sample of ETGs from the SPIDER project and found compelling evidence for heavier IMFs in the central regions of higher-$\sigma_\star$ galaxies. The IMF mismatch relative to Chabrier is $\delta_{IMF} \sim$ 0.5–1.1 at $\sigma_\star \sim$ 125 km s^{-1} and $\sim$1.2–1.8 at $\sim$250 km s^{-1}. The δ_{IMF}–$\sigma_\star$ trend is robust to a wide set of modeling assumptions and accounts for much of the tilt in the fundamental plane. The distribution of DM is degenerate with the overall IMF normalization and difficult to constrain, and therefore we have assumed that any halo contraction is invariant with $\sigma_\star$. Some ways to break the degeneracy between IMF and halo contraction are to (1) analyze cases with extended velocity dispersion or X-ray emission profiles (e.g., Napolitano et al. 2009, 2011) or (2) incorporate complementary data from strong/ weak gravitational lensing (e.g., Auger et al. 2010). However, we have argued that the only way to preserve the IMF universality is to allow for halo contraction at high $\sigma_\star$ and halo *expansion* at low $\sigma_\star$.

We have performed the first general inventory of IMF results from a variety of studies in the literature, using both pure and hybrid techniques, and found that these generally agree well with our SPIDER results. There is remarkably widespread agreement on a Salpeter-like IMF for massive ETGs ($\sigma_\star \gtrsim$ 200 km s^{-1}). At lower $\sigma_\star$, the data are still somewhat limited and the different results have not yet converged, but most of the studies point to MW-like IMFs. Agreement on a super-Salpeter IMF in the most massive galaxies ($\sigma_\star \gtrsim$ 275 km s^{-1}) is also not yet universal.

These results appear to be fully compatible with underlying ΛCDM halos. However, more detailed conclusions about halo contraction or expansion are still elusive, and the data on galaxy centers do not clearly rule out alternative DM models once the variable IMF is accounted for.

More work is clearly needed to understand the systematics in the different analyses; to build up better statistics on a wide range of galaxy types, environments, and redshifts; and to determine which parameters correlate best with IMF variations (e.g., metallicity or starburst intensity; CvD12; Smith et al. 2012). It may also be particularly helpful to venture beyond the centers of galaxies, using data from a wide baseline in radius to help break the IMF–DM degeneracies.

It appears we are nearing convergence on determining *what* the basic components of galaxies are (distributions of stars and DM). The next challenge will be to understand *why* these arrive at their distributions. What drives the power spectrum in cloud fragmentation and star formation? How do baryonic processes interact with and re-shape their surrounding DM halos?

REFERENCES

Abadi, M. G., Navarro, J. F., Fardal, M., Babul, A., & Steinmetz, M. 2010, MNRAS, 407, 435 (A+10)
Auger, M. W., Treu, T., Gavazzi, R., et al. 2010, ApJL, 721, L163
Barnabè, M., Dutton, A. A., Marshall, P. J., et al. 2012, MNRAS, 423, 1073 (B+12)
Bastian, N., Covey, K. R., & Meyer, M. R. 2010, ARA&A, 48, 339
Bell, E. F., & de Jong, R. S. 2001, ApJ, 550, 212
Bershady, M. A., Martinsson, T. P. K., Verheijen, M. A. W., et al. 2011, ApJL, 739, L47
Blumenthal, G. R., Faber, S. M., Flores, R., & Primack, J. R. 1986, ApJ, 301, 27 (B+86)
Brewer, B. J., Dutton, A. A., Treu, T., et al. 2012, MNRAS, 422, 3574
Bruzual, G., & Charlot, S. 2003, MNRAS, 344, 1000
Burkert, A. 1995, ApJL, 447, L25
Cappellari, M., Bacon, R., Bureau, M., et al. 2006, MNRAS, 366, 1126 (C+06)
Cappellari, M., di Serego Alighieri, S., Cimatti, A., et al. 2009, ApJL, 704, L34
Cappellari, M., McDermid, R. M., Alatalo, K., et al. 2012a, Natur, 484, 485
Cappellari, M., McDermid, R. M., Alatalo, K., et al. 2012b, MNRAS, submitted (arXiv:1208.3523) (C+12)
Carter, D., Visvanathan, N., & Pickles, A. J. 1986, ApJ, 311, 637
Cenarro, A. J., Gorgas, J., Vazdekis, A., Cardiel, N., & Peletier, R. F. 2003, MNRAS, 339, L12
Chabrier, G. 2003, PASP, 115, 763
Conroy, C., & van Dokkum, P. G. 2012, ApJ, 760, 71
de Blok, W. J. G., Walter, F., Brinks, E., et al. 2008, AJ, 136, 2648
de Vaucouleurs, G. 1948, AnAP, 11, 247
Dutton, A. A., Brewer, B. J., Marshall, P. J., et al. 2011, MNRAS, 417, 1621
Dutton, A. A., Maccio', A. V., Mendel, J. T., & Simard, L. 2012a, MNRAS, submitted (arXiv:1204.2825) (D+12a)
Dutton, A. A., Mendel, J. T., & Simard, L. 2012b, MNRAS, 422, L33
Dutton, A. A., Treu, T., Brewer, B. J., et al. 2013, MNRAS, 428, 3183 (D+13)
Falcón-Barroso, J., Peletier, R. F., Vazdekis, A., & Balcells, M. 2003, ApJL, 588, L17
Ferreras, I., La Barbera, F., de Carvalho, R. R., et al. 2013, MNRAS, 429, L15
Ferreras, I., Saha, P., & Burles, S. 2008, MNRAS, 383, 857
Ferreras, I., Saha, P., Leier, D., Courbin, F., & Falco, E. E. 2010, MNRAS, 409, L30 (F+10)
Gnedin, O. Y., Kravtsov, A. V., Klypin, A. A., & Nagai, D. 2004, ApJ, 616, 16 (G+04)
Grillo, C. 2010, ApJ, 722, 779
Grillo, C., & Gobat, R. 2010, MNRAS, 402, L67
Kroupa, P. 2001, MNRAS, 322, 231
Kroupa, P., Weidner, C., Pflamm-Altenburg, J., et al. 2011, arXiv:1112.3340
La Barbera, F., de Carvalho, R. R., de La Rosa, I. G., & Lopes, P. A. A. 2010a, MNRAS, 408, 1335
La Barbera, F., de Carvalho, R. R., de La Rosa, I. G., et al. 2010b, MNRAS, 408, 1313
La Barbera, F., de Carvalho, R. R., Kohl-Moreira, J. L., et al. 2008, PASP, 120, 681
La Barbera, F., Lopes, P. A. A., de Carvalho, R. R., de La Rosa, I. G., & Berlind, A. A. 2010c, MNRAS, 408, 1361
Macciò, A. V., Dutton, A. A., & van den Bosch, F. C. 2008, MNRAS, 391, 1940
Milgrom, M. 1983, ApJ, 270, 371
Moster, B. P., Somerville, R. S., Maulbetsch, C., et al. 2010, ApJ, 710, 903 (M+10)
Napolitano, N. R., Romanowsky, A. J., Capaccioli, M., et al. 2011, MNRAS, 411, 2035 (N+11)
Napolitano, N. R., Romanowsky, A. J., Coccato, L., et al. 2009, MNRAS, 393, 329 (N+09)
Napolitano, N. R., Romanowsky, A. J., & Tortora, C. 2010, MNRAS, 405, 2351
Navarro, J. F., Frenk, C. S., & White, S. D. M. 1996, ApJ, 462, 563
Salpeter, E. E. 1955, ApJ, 121, 161

Schneider, A., Smith, R. E., Macciò, A. V., & Moore, B. 2012, MNRAS, 424, 684 (S+12a)

Schulz, A. E., Mandelbaum, R., & Padmanabhan, N. 2010, MNRAS, 408, 1463

Smith, R. J., Lucey, J. R., & Carter, D. 2012, MNRAS, 426, 2994 (S+12b)

Sonnenfeld, A., Treu, T., Gavazzi, R., et al. 2012, ApJ, 752, 163 (S+12c)

Spiniello, C., Koopmans, L. V. E., Trager, S. C., Czoske, O., & Treu, T. 2011, MNRAS, 417, 3000

Spiniello, C., Trager, S. C., Koopmans, L. V. E., & Chen, Y. P. 2012, ApJL, 753, L32

Suyu, S. H., Hensel, S. W., McKean, J. P., et al. 2012, ApJ, 750, 10

Swindle, R., Gal, R. R., La Barbera, F., & de Carvalho, R. R. 2011, AJ, 142, 118

Thomas, J., Saglia, R. P., Bender, R., et al. 2011, MNRAS, 415, 545 (T+11)

Tortora, C., La Barbera, F., Napolitano, N. R., de Carvalho, R. R., & Romanowsky, A. J. 2012, MNRAS, 425, 577

Tortora, C., Napolitano, N. R., Romanowsky, A. J., Capaccioli, M., & Covone, G. 2009, MNRAS, 396, 1132

Tortora, C., Napolitano, N. R., Romanowsky, A. J., & Jetzer, P. 2010, ApJL, 721, L1

Treu, T., Auger, M. W., Koopmans, L. V. E., et al. 2010, ApJ, 709, 1195 (T+10)

van Dokkum, P. G., & Conroy, C. 2010, Natur, 468, 940

Wegner, G. A., Corsini, E. M., Thomas, J., et al. 2012, AJ, 144, 78 (W+12)

Westfall, K. B., Bershady, M. A., Verheijen, M. A. W., et al. 2011, ApJ, 742, 18